Table V. Best Results of Orpen Calculations: Fractional Positions, Bond Lengths (Å), and Potential Energies (eV)

bond length					fractional position			
Pt-H	Au-H				*x*	*y*	*z*	energy
1.86	Au(5)	1.83	Au(8)	1.82	-0.0282	0.5879	0.3084	0.54
1.85	Au(4)	1.82	Au(5)	1.82	0.1204	0.6029	0.3157	1.01
1.86	Au(3)	1.82	Au(4)	1.82	0.1281	0.5447	0.3162	1.16
1.86	Au(2)	1.81	Au(6)	1.81	-0.0649	0.3887	0.2971	1.99
1.85	Au(2)	1.80	Au(3)	1.80	-0.0007	0.3986	0.3011	2.46

respectively, for a reasonable yield. Unprotonated $Pt(PPh_3)(AuPPh_3)_7^+$ could not be detected.

$$Pt(AuPPh_3)_8^{2+} + H^+ + 2PPh_3 \rightarrow Pt(H)(PPh_3)(AuPPh_3)_7^{2+} + Au(PPh_3)_2^+ \quad (3)$$

$$Pt(H)(PPh_3)(AuPPh_3)_7^{2+} + NEt_3 + 2AuPPh_3^+ \rightarrow Pt(AuPPh_3)_8^{2+} + HNEt_3^+ + Au(PPh_3)_2^+ \quad (4)$$

The presence of H in the Pt-Au cluster compound is firmly established by FABMS and NMR data. The asymmetric positions of the Au atoms around the central Pt give an indication where this H could be located. A method for the location of hydride ligands has been developed by Orpen.[21] On the basis of the X-ray-determined coordinates of the non-hydrogen atoms, the potential energy is minimized by varying the hydride position. For a large variety of clusters this method has proven to be useful in determining hydride positions.[22,23] For $Pt(H)(PPh_3)(AuPPh_3)_7^{2+}$ the best solutions are obtained if bonding interactions of H with Pt and two Au atoms (facial bridging μ_3-coordination) are allowed. The five best solutions are given in Table V. The lowest potential energy corresponds with H μ_3-bonded to Pt, Au(5), and Au(8), and this is in accord with the conclusions given above, concerning bonding lengths around Au(5) and Au(8), the high ^{195}Pt-H coupling constant, and the intensity ratio of 2:5 for the two quadrupole pairs in the Mössbauer spectrum. In a simple approximation of the HOMO of $Pt(PPh_3)(AuPPh_3)_7^+$, which lacks the H atom, using X-ray-determined coordinates and an EHMO calculation, the maximum electron density was found in a lobe pointing toward Au(6) and Au(8). This suggests that H should be bonded near that region. Although all these arguments do not give an accurate position of H, we can safely conclude that it is positioned within the area defined by Pt, Au(5), Au(6), and Au(8).

In the very few other known hydride complexes of gold, the hydride is μ_2-bridging between Au and Pt, Ir, Ru, Cr, or W.[23,24]

The Pt-P bonding distance is relatively large and suggests a loosely bonded phosphine. The reactivity caused by loosely bonded phosphine is well-known,[24] e.g. for $Au(PPh_3)(AuPPh_3)_7^{2+}$,[3] and is currently being explored for $Pt(H)(PPh_3)(AuPPh_3)_7^{2+}$.

Acknowledgment. We thank Dr. H. H. A. Smit and Dr. R. C. Thiel of the Kamerlingh Onnes Laboratory in Leiden for recording the Mössbauer spectrum. This investigation was supported by the Netherlands Foundation for Chemical Research (SON) and by a National Science Foundation grant to L.H.P.

Supplementary Material Available: Tables of experimental details for the X-ray diffraction study, anisotropic temperature factors, fractional positional and thermal parameters of the phenyl atoms and dichloromethane atoms, and fractional positional and occupation parameters of the fluoride atoms (9 pages); a table of calculated and observed structure factors (81 pages). Ordering information is given on any current masthead page.

(21) Orpen, A. G. *J. Chem. Soc., Dalton Trans.* **1980**, 2509.
(22) Henrick, K.; McPartlin, M.; Morris, J. *Angew. Chem., Int. Ed. Engl.* **1976**, *25*, 853.
(23) Mueting, A. M.; Bos, W.; Alexander, B. D.; Boyle, P. D.; Casalnuovo, J. A.; Balaban, S.; Ito, L. N.; Johnson, S. M.; Pignolet, L. H. *New J. Chem.*, in press.
(24) Puddephatt, R. J. In *Comprehensive Coordination Chemistry*; Wilkinson, G., Ed.; Pergamon: Oxford, England, 1987; Vol. 5, p 861.

Contribution from the Department of Chemistry, Southern Methodist University, Dallas, Texas 75275

Reactions of a Phosphoranide Platinum(II) Complex with Nucleophilic and Electrophilic Reagents and the X-ray Crystal Structures of (η^2-cyclenP)Pt[Co(CO)$_4$]PPh$_3$ and (η^2-cyclenP)Pt(I)PPh$_3$

Dilip V. Khasnis, Michael Lattman,* and Upali Siriwardane

Received November 8, 1988

The reactions of the phosphoranide-containing complex (η^2-cyclenP)Pt(Cl)PPh$_3$ (**1**) with a variety of nucleophiles and electrophiles have been studied. These reactions demonstrate the remarkable range and selectivity of this complex. With the anionic nucleophiles $Co(CO)_4^-$, SMe^-, I^-, and Br^-, the corresponding chloride-substituted derivatives are formed, (η^2-cyclenP)PtLPPh$_3$, where L = $Co(CO)_4$ (**5**), SMe (**6**), I (**7**), and Br (**8**). The neutral, potentially bidentate, donor dppm leads to PPh_3 substitution to give (η^2-cyclenP)Pt(Cl)dppm (**9**), where only one of the phosphorus sites of dppm is bound to the platinum. The electrophiles MeI and *n*-BuBr also lead to **7** and **8**. However, the reaction of MeO_3SCF_3 with **1** led to [(η^2-MecyclenP)Pt(Cl)PPh$_3$]O_3SCF_3 (**10**), where the platinum-bound nitrogen is methylated and the P-N bond is cleaved. This suggests that the alkyl halide reactions may proceed through such an intermediate, rather than the usual oxidative-addition/reductive-elimination path. The reaction of **1** with HC≡CPh and $NaBPh_4$ leads to the σ-bonded alkyne complex [(η^2-HcyclenP)Pt(C≡CPh)PPh$_3$]BPh_4 (**11**), where both P-N bond cleavage and chloride substitution has occurred. Reaction of **5** and Me_3SiI leads to **7** and $Me_3SiCo(CO)_4$. The X-ray crystal structures of **5** and **7** were obtained and show extremely long Pt-Co and Pt-I bonds, respectively. X-ray data: $C_{30}H_{31}N_4O_4P_2CoPt$ (**5**), triclinic, space group $P\bar{1}$, a = 10.374 (4) Å, b = 10.857 (6) Å, c = 16.086 (9) Å, α = 78.93 (4)°, β = 83.31 (4)°, γ = 61.93 (3)°, Z = 2, R = 0.059, R_w = 0.060; $C_{26}H_{31}N_4P_2IPt$ (**7**), monoclinic, space group $P2_1/c$, a = 11.939 (5) Å, b = 14.446 (5) Å, c = 15.407 (9) Å, β = 92.80 (4)°, Z = 4, R = 0.053, R_w = 0.064.

Reactions at square-planar platinum(II) centers are important due to their central role in catalysis, which include activation of C-H bonds and fundamental aspects of oxidative addition and reductive elimination.[1] In addition, metal complexes containing

0020-1669/89/1328-2594$01.50/0

Scheme I

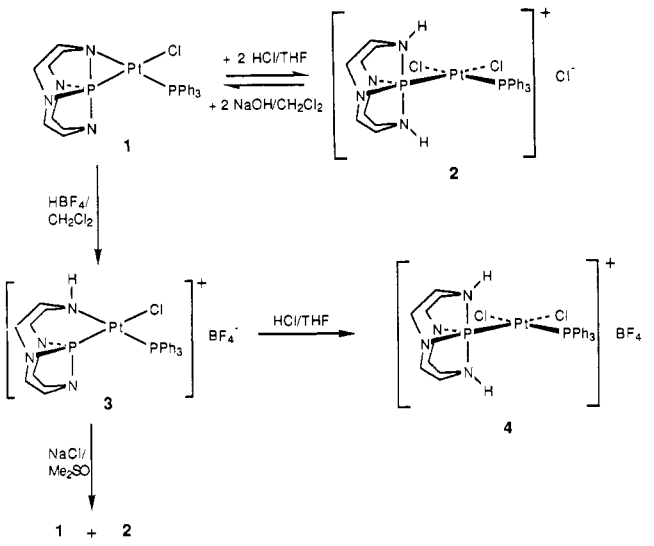

macrocyclic amine ligands have also found use in biochemical applications.[2] We have recently reported the synthesis and preliminary reactivity of (η^2-cyclenP)Pt(Cl)PPh_3 (**1**) and related

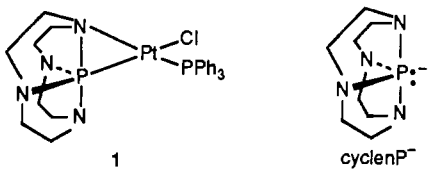

derivatives,[3] which incorporate a macrocyclic amine-containing phosphoranide (R_4P:$^-$) ligand[4] on a platinum(II) site. These systems are important since they are capable of altering the reactions and mechanistic pathways of platinum complexes due to the presence of basic nitrogens on the ligand. We have already demonstrated that very strong electrophiles, such as protic acids, attack the cyclenP ligand rather than undergo the usual oxidative addition to platinum.[3b,c] These are summarized in Scheme I. Thus, reaction of **1** with HCl leads directly to **2**, while treatment of **2** with NaOH re-forms **1**. The most likely intermediate in these reactions, **3**, was isolated with HBF_4.

We now report a systematic investigation of the reactivity of **1** with a variety of nucleophiles and electrophiles. This study demonstrates that different reactive sites can be selectively attacked by suitable choices of reagents. Moreover, while nucleophiles result in a variety of substitution products, including heterobimetallics, evidence suggests that electrophiles initially lead to P–N bond cleavage at cyclenP.

Experimental Section

All reactions and manipulations were carried out under an atmosphere of nitrogen in a Vacuum Atmospheres Model DL-001-S-P drybox or with use of standard Schlenk techniques, unless otherwise indicated. Solvents were dried and distilled under a nitrogen atmosphere and either used immediately or stored in the drybox prior to use. Glassware was oven-dried at 140 °C overnight prior to use. The reagents MeO_3SCF_3, MeI, *n*-BuBr, $Co_2(CO)_8$, NaSMe, $CH_2(PPh_2)_2$ (dppm), KI, KBr, $NaBPh_4$, and HC≡CPh were obtained commercially and used without further purification except for $Co_2(CO)_8$ (sublimed) and HC≡CPh (distilled). **1** was prepared by the literature method.[3b,c] All NMR spectra were recorded on an IBM/Bruker WP200SY multinuclear NMR spectrometer resonating at 200.132 (^{1}H), 81.026 (^{31}P), and 50.327 (^{13}C) MHz. ^{31}P and ^{13}C spectra are proton-decoupled unless otherwise indicated. ^{1}H resonances were measured relative to residual proton solvent peaks, referenced to Me_4Si; ^{13}C resonances were measured relative to solvent peaks, referenced to Me_4Si; ^{31}P resonances were measured relative to external 85% H_3PO_4. Melting points were obtained in nitrogen-filled tubes on a Mel-Temp capillary apparatus and are uncorrected. Elemental analyses were obtained on a Carlo Erba Strumentazione Model 1106 elemental analyzer.

Synthesis of (η^2-cyclenP)Pt[Co(CO)$_4$]PPh_3 (5). Na[Co(CO)$_4$] was prepared by a literature method[5] using NaOH (100 mg, 2.50 mmol) and $Co_2(CO)_8$ (68 mg, 0.20 mmol) in THF (5 mL). The resulting solution was filtered and added dropwise to solid **1** (204 mg, 0.295 mmol). The reaction mixture turned yellow immediately and was then stirred and monitored by ^{31}P NMR and IR spectroscopy. After 4 h, the spectra showed the reaction to be complete. The mixture was then filtered. Hexane was layered on top of the THF solution and allowed to slowly diffuse in, yielding yellow, air-stable crystals of **5** (176 mg, 72%), dec pt 183–185 °C. Anal. Calcd for $C_{30}H_{31}CoN_4O_4P_2Pt$: C, 43.55; H, 3.75; N, 6.78. Found: C, 43.67; H, 3.94; N, 6.87. ^{13}C{^{1}H} NMR for cyclen ring (THF-d_8; ppm): 44.4 (d, $^2J_{PC}$ = 15 Hz), 44.7 (d, $^2J_{PC}$ = 10 Hz), 48.0, 51.3; 213.7 (br, CO). ν_{CO} (THF; cm^{-1}): 1885 vs, 1920 sh, 1943 s, 2018 m. ν_{CO} (Nujol, cm^{-1}): 1883 vs, 1905 vs, 1938 vs, 2017 s.

Synthesis of (η^2-cyclenP)Pt(SMe)PPh_3 (6). A mixture of **1** (250 mg, 0.360 mmol) and NaSMe (25 mg, 0.36 mmol) in THF (10 mL) was stirred for 12 h. After filtration, the volatiles were pumped off. The residue was redissolved in THF. Hexane was layered on top of the solution and allowed to slowly diffuse in, yielding pale yellow, air-stable crystals of **6** (240 mg, 94%), dec pt 238–240 °C. Anal. Calcd for $C_{27}H_{34}N_4P_2PtS$: C, 46.05; H, 4.83; N, 7.95. Found: C, 46.20; H, 4.64; N, 7.82.

Synthesis of (η^2-cyclenP)Pt(I)PPh_3 (7) by Reaction of 1 with MeI. A stirred solution of **1** (100 mg, 0.145 mmol) in THF (4 mL) was treated dropwise with MeI (10 μL, 0.15 mmol). A white precipitate formed immediately. The reaction mixture was stirred for 12 h. The solid was collected by filtration, dried, and dissolved in CH_2Cl_2 (3 mL). Diethyl ether was layered on top and allowed to slowly diffuse in, yielding white, air-stable crystals of **7** (113 mg, 96%), dec pt 210–212 °C. Anal. Calcd for $C_{26}H_{31}IN_4P_2Pt$: C, 39.87; H, 3.95; N, 7.15. Found: C, 39.23; H, 4.05; N, 7.24. ^{13}C{^{1}H} NMR for cyclen ring (CD_2Cl_2; ppm): 44.6 (d, $^2J_{PC}$ = 15 Hz), 44.7 (d, $^2J_{PC}$ = 10 Hz), 47.2, 51.2.

Synthesis of (η^2-cyclenP)Pt(Br)PPh_3 (8) by Reaction of 1 with *n*-BuBr. An excess of *n*-BuBr (0.25 mL, 2.6 mmol) was added dropwise to a stirred solution of **1** (69 mg, 0.10 mmol) in CH_2Cl_2 (1 mL). The progress of the reaction was followed by ^{31}P NMR spectroscopy. Spectra showed the reaction to be complete after 72 h. The volatiles were pumped off, and the resulting solid was washed with diethyl ether, yielding white, air-stable crystals of **8** (70 mg, 94%), dec pt 230–232 °C. Anal. Calcd for $C_{26}H_{31}BrN_4P_2Pt$: C, 42.36; H, 4.20; N, 7.60. Found: C, 41.69; H, 4.25; N, 7.65. ^{13}C{^{1}H} NMR for cyclen ring ($CDCl_3$; ppm): 44.6 (d, $^2J_{PC}$ = 17 Hz), 45.1 (d, $^2J_{PC}$ = 10 Hz), 47.3, 50.4.

Synthesis of 7 by Reaction of 1 with KI. A mixture of **1** (69 mg, 0.10 mmol) and KI (20 mg, 0.12 mmol) in CH_2Cl_2 (3 mL) was stirred and the progress of the reaction followed by ^{31}P NMR spectroscopy. Spectra showed the reaction to be complete after 48 h. The mixture was then filtered to remove a small amount of solid, and the volatiles were pumped off from the filtrate to yield spectroscopically pure **7** (74 mg, 93%).

Synthesis of 8 by Reaction of 1 with KBr. A mixture of **1** (69 mg, 0.10 mmol) and KBr (12 mg, 0.10 mmol) in CH_2Cl_2 (2 mL) was stirred and the progress of the reaction followed by ^{31}P NMR spectroscopy. Spectra showed the reaction to be complete after 72 h. The mixture was then filtered to remove a small amount of solid, and the volatiles were pumped off from the filtrate to yield spectroscopically pure **8** (72 mg, 98%).

Synthesis of (η^2-cyclenP)Pt(Cl)dppm (9). A stirred solution of **1** (138 mg, 0.200 mmol) in THF (2 mL) was treated dropwise with a solution of dppm (80 mg, 0.21 mmol) in THF (1 mL). Stirring was continued for 8 h, after which the volatiles were pumped off. The residue was washed with hexane to remove free PPh_3 and the resulting solid redissolved in THF. Diethyl ether was layered on top of the solution and

(1) (a) Hartley, F. R. In *Comprehensive Organometallic Chemistry*; Wilkinson, G., Stone, F. G. A., Abel, E. W., Eds.; Pergamon: Oxford, 1982; Vol. 6, p 471. (b) Hartley, F. R. *The Chemistry of Platinum and Palladium*; Applied Science: London, 1973. (c) Ciapetta, F. G.; Wallace, D. N. *Catal. Rev.* **1971**, *5*, 67. (d) Crespo, M.; Puddephatt, R. J. *Organometallics* **1987**, *6*, 2548.

(2) (a) Kimura, E.; Korenari, S.; Shionoya, M.; Shiro, M. *J. Chem. Soc., Chem. Commun.* **1988**, 1166. (b) Moi, M. K.; Yanuck, M.; Deshpande, S. V.; Hope, H.; DeNardo, S. J.; Meares, C. F. *Inorg. Chem.* **1987**, *26*, 3458.

(3) (a) Lattman, M.; Chopra, S. K.; Burns, E. G. *Phosphorus Sulfur* **1987**, *30*, 185. (b) Lattman, M.; Burns, E. G.; Chopra, S. K.; Cowley, A. H.; Arif, A. M. *Inorg. Chem.* **1987**, *26*, 1926. (c) Khasnis, D. V.; Lattman, M.; Siriwardane, U. *Inorg. Chem.* **1989**, *28*, 681.

(4) (a) Burns, E. G.; Chu, S. S. C.; de Meester, P.; Lattman, M. *Organometallics* **1986**, *5*, 2383. (b) Lattman, M.; Chopra, S. K.; Cowley, A. H.; Arif, A. M. *Organometallics* **1986**, *5*, 677. (c) de Meester, P.; Lattman, M.; Chu, S. S. C. *Acta Crystallogr., Sect. C* **1987**, *C43*, 162. (d) Lattman, M.; Olmstead, M. M.; Power, P. P.; Rankin, D. W.; Robertson, H. E. *Inorg. Chem.* **1988**, *27*, 3012.

(5) (a) Edgell, W. F.; Lyford, J., IV. *Inorg. Chem.* **1970**, *9*, 1932. (b) Matachek, J. R.; Angelici, R. J.; Schugart, K. A.; Haller, K. J.; Fenske, R. F. *Organometallics* **1984**, *3*, 1038.

Table I. Crystallographic Data for **5** and **7**

	5	**7**
chem formula	$C_{30}H_{31}N_4O_4P_2CoPt$	$C_{26}H_{31}N_4P_2IPt$
a, Å	10.374 (4)	11.939 (5)
b, Å	10.857 (6)	14.446 (5)
c, Å	16.086 (9)	15.407 (9)
α, deg	78.93 (4)	
β, deg	83.31 (4)	92.80 (4)
γ, deg	61.93 (3)	
V, Å^3	1565 (1)	2654 (2)
Z	2	4
fw	872.61	783.54
space group	$P\bar{1}$ (No. 2)	$P2_1/c$ (No. 14)
T, °C	26	26
λ, Å	0.71073	0.71073
ρ_{calcd}, g cm^{-3}	1.76	1.96
μ, cm^{-1}	0.518	0.663
transmissn coeff	1.00–0.578	0.963–0.678
R^a	0.059	0.053
R_w	0.060	0.064

$^a R = \sum||F_o| - |F_c||/\sum w|F_o|$, $R_w = [w(F_o - F_c)^2/\sum(F_o)^2]^{1/2}$, and $w = 1/\sigma^2(F_o) + k(F_o)^2$.

allowed to slowly diffuse in, yielding white, air-stable crystals of **9** (150 mg, 92%), mp 170–172 °C. Anal. Calcd for $C_{33}H_{38}ClN_4P_3Pt$: C, 48.69; H, 4.66; N, 6.88. Found: C, 48.68; H, 4.65; N, 7.10. $^{13}C\{^1H\}$ NMR for cyclen ring (THF-d_8; ppm): 47.2 (d, $^2J_{PC}$ = 18 Hz), 47.8 (d, $^2J_{PC}$ = 20 Hz), 51.2, 52.7.

Synthesis of [(η²-MecyclenP)Pt(Cl)PPh₃]O₃SCF₃ (10). A solution of **1** (100 mg, 0.145 mmol) in CH_2Cl_2 was kept at −35 °C in the drybox freezer overnight. After this solution was removed from the freezer, MeO_3SCF_3 (16.5 μL, 0.145 mmol) was immediately added dropwise while stirring. The reaction mixture was stirred at room temperature for 4 h. At this time, the ^{31}P NMR spectrum indicated the reaction to be complete; however, some small-intensity peaks due to impurities were present in the spectrum. The volatiles were then pumped off, and the resulting solid was washed with diethyl ether and dried to yield **10** as an impure, pale yellow solid (110 mg, 90%), mp 140–142 °C. Attempts at further purification were unsuccessful since the product is unstable in solution and decomposes quickly in THF and $CDCl_3$ but more slowly in CH_2Cl_2. $^{13}C\{^1H\}$ NMR for cyclen ring (CD_2Cl_2; ppm): 45.9 (d, $^2J_{PC}$ = 7 Hz), 49.7, 52.9, 62.6; 58.6 (Me). In an off-resonance decoupling experiment, the last resonance splits into a quartet, while the others split into triplets, confirming the assignments. The reaction of **1** with Me_3OBF_4 was carried out to see if the BF_4 anion might lead to a cleaner synthesis; this was unsuccessful.

Reaction of 10 with KI. A mixture of **10** (85 mg, 0.10 mmol) and KI (16 mg, 0.10 mmol) in THF (2 mL) was stirred for 16 h. The resulting white precipitate was dried (70 mg) and redissolved in CH_2Cl_2 (1 mL). The ^{31}P NMR spectrum of this solution indicated the presence of **7**, along with several impurities. Peak intensities indicated about a 30–35% yield of **7**.

Synthesis of [(η²HcyclenP)Pt(C≡CPh)PPh₃]BPh₄ (11). A slurry of **1** (69 mg, 0.10 mmol), HCCPh (25 μL, 0.22 mmol), and $NaBPh_4$ (34 mg, 0.10 mmol) in diethyl ether (3 mL) was stirred for 24 h. The resulting white solid was filtered and then washed with CH_2Cl_2 to dissolve the product. The CH_2Cl_2 solution was then filtered (to remove NaCl), and the volatiles were pumped off, yielding **10** as an air-stable, white solid (95 mg, 88%), dec pt 214–216 °C. Anal. Calcd for $C_{58}H_{57}N_4P_2Pt$: C, 64.58; H, 5.29; N, 5.79. Found: C, 63.68; H, 5.43; N, 5.43. The product decomposes slowly in solution. $^{13}C\{^1H\}$ NMR for cyclen ring (CD_2Cl_2): 45.7 (d, $^2J_{PC}$ = 5 Hz), 49.7 (d, $^2J_{PC}$ = 5 Hz), 50.2, 52.8; 107.7, 108.6 (C≡C).[6] $\nu_{C\equiv C}$ (Nujol; cm^{-1}): 2105.

Reaction of 5 with Me_3SiI. Me_3SiI (4 μL, 0.05 mmol) was added dropwise to a stirred slurry of **5** (40 mg, 0.050 mmol) in cyclohexane-d_{12}. After 8 h of stirring, the resulting white precipitate was filtered, washed with THF, and pumped dry to yield spectroscopically pure **7** (34 mg, 91%). The proton NMR spectrum of the cyclohexane-d_{12} supernatant showed one peak at δ 0.60, in agreement with that previously reported for $Me_3SiCo(CO)_4$.[7]

X-ray Structure Determination and Refinement. Dark yellow crystals of **5** were grown by slow diffusion of hexane into a THF solution of **5**. Colorless crystals of **7** were grown by slow diffusion of hexane into a methylene chloride solution of **7**. Crystals were mounted on an automatic Nicolet R3m/v diffractometer for data collection. The pertinent crystallographic data are summarized in Table I. The unit cell parameters were determined by a least-squares fit of 25 reflections in the range $15 < 2\theta < 25°$. Three standard reflections were remeasured after every 100 reflections during the data collection. The space group assignments were consistent with the systematic absences. All data were corrected for decay and Lorentz–polarization effects. Data were corrected for absorption on the basis of ψ scans. The structures were solved by direct methods using SHELXTL-PLUS[8] and subsequent difference Fourier methods. Neutral-atom scattering factors and corrections for anomalous dispersion were from common sources.[9] Full-matrix least-squares refinements were carried out by using only the observed reflections $F > 6.0\sigma(F)$, the function minimized being $\sum w(|F_o| - |F_c|)^2$. All non-hydrogen atoms were refined anisotropically; hydrogens on carbon atoms were included in calculated positions by using a riding model with fixed isotropic parameters.

Atomic coordinates and equivalent isotropic thermal parameters for **5** and **7** are given in Tables II and III, respectively.

Table II. Atomic Coordinates (×10⁴) and Equivalent Isotropic Displacement Parameters (Å² × 10³) for **5**

	x	y	z	U(eq)^a
Pt	2516 (1)	1926 (1)	2788 (1)	31 (1)
Co	3417 (2)	−707 (2)	2402 (1)	47 (1)
P(1)	910 (3)	3662 (3)	3415 (2)	35 (1)
P(2)	4046 (3)	2732 (3)	2239 (2)	30 (1)
N(1)	700 (10)	2024 (11)	3472 (7)	45 (5)
N(2)	−718 (9)	4620 (9)	2871 (6)	42 (4)
N(3)	1109 (11)	5125 (10)	3393 (6)	44 (4)
N(4)	1256 (12)	3167 (10)	4497 (6)	50 (5)
O(1)	1488 (12)	1583 (12)	1009 (7)	79 (6)
O(2)	1518 (15)	−1684 (14)	3402 (10)	108 (8)
O(3)	5341 (14)	−2802 (14)	1432 (9)	100 (7)
O(4)	5577 (13)	−964 (11)	3633 (8)	93 (6)
C(1)	2243 (19)	740 (16)	1591 (9)	59 (8)
C(2)	2267 (19)	−1314 (14)	2996 (10)	74 (8)
C(3)	4592 (19)	−2003 (16)	1818 (10)	71 (8)
C(4)	4682 (17)	−758 (15)	3138 (9)	61 (7)
C(5)	−642 (15)	2359 (17)	2971 (10)	60 (8)
C(6)	−1188 (14)	3872 (16)	2408 (10)	65 (8)
C(7)	−1085 (13)	6081 (12)	2460 (10)	61 (6)
C(8)	−41 (15)	6440 (13)	2846 (9)	61 (6)
C(9)	1557 (15)	5275 (13)	4212 (8)	51 (6)
C(10)	2029 (13)	3879 (13)	4794 (8)	56 (6)
C(11)	1746 (16)	1696 (16)	4819 (8)	57 (8)
C(12)	933 (15)	1247 (13)	4323 (9)	64 (7)
C(13)	3153 (11)	4279 (11)	1377 (7)	37 (4)
C(14)	3923 (14)	5011 (12)	990 (7)	48 (5)
C(15)	3204 (13)	6215 (14)	337 (8)	58 (6)
C(16)	1793 (15)	6636 (15)	45 (9)	65 (7)
C(17)	1064 (17)	5905 (16)	367 (9)	72 (7)
C(18)	1788 (14)	4681 (14)	1055 (8)	52 (6)
C(19)	4804 (12)	3213 (12)	3053 (7)	37 (5)
C(20)	4696 (13)	4571 (14)	2982 (10)	50 (6)
C(21)	5338 (15)	4830 (16)	3630 (11)	67 (8)
C(22)	6071 (15)	3802 (19)	4351 (11)	65 (9)
C(23)	6156 (13)	2439 (15)	4423 (9)	60 (7)
C(24)	5518 (13)	2182 (12)	3793 (7)	47 (6)
C(25)	5631 (11)	1562 (11)	1745 (6)	32 (4)
C(26)	5387 (11)	1138 (13)	1005 (8)	52 (5)
C(27)	6528 (15)	279 (16)	613 (8)	67 (7)
C(28)	7961 (15)	−244 (14)	904 (9)	61 (6)
C(29)	8244 (13)	166 (15)	1633 (9)	64 (6)
C(30)	7081 (13)	1031 (14)	2054 (9)	54 (6)

^{a} Equivalent isotropic U defined as one-third of the trace of the orthogonalized U_{ij} tensor.

Results and Discussion

Reactions. The nucleophilic reactions appear to be more straightforward and will be discussed first. Reactions of **1** with

(6) The ^{13}C values for C≡C in **11** agree well with other Pt—C≡C data: Sebald, A.; Wrackmeyer, B.; Beck, W. *Z. Naturforsch.* **1983**, *38B*, 45. J_{PtC} values for these carbons could not be obtained due to very low signal intensities.

(7) Baay, Y. L.; MacDiarmid, A. G. *Inorg. Chem.* **1969**, *8*, 986.

(8) Sheldrick, G. M. "SHELXTL-Plus88, Structure Determination Software Programs"; Nicolet Instrument Corp.: 5225-5 Verona Road, Madison, WI 53711, 1988.

(9) "International Tables for X-ray Crystallography"; Kynoch Press: Birmingham, England, 1974; Vol. IV.

Table III. Atomic Coordinates ($\times 10^4$) and Equivalent Isotropic Displacement Parameters ($Å^2 \times 10^3$) for **7**

	x	y	z	U(eq)[a]
Pt	2024 (1)	1998 (1)	1829 (1)	25 (1)
I	−196 (1)	2423 (1)	1491 (1)	46 (1)
P(1)	3258 (2)	1285 (2)	2751 (2)	27 (1)
P(2)	2818 (2)	2332 (2)	584 (2)	25 (1)
N(1)	1786 (7)	1442 (6)	3072 (5)	30 (2)
N(2)	3662 (9)	1953 (6)	3624 (7)	38 (3)
N(3)	4644 (7)	1077 (8)	2525 (6)	43 (3)
N(4)	2980 (8)	110 (6)	2706 (6)	39 (3)
C(1)	1696 (12)	2098 (10)	3806 (8)	51 (5)
C(2)	2805 (11)	2572 (9)	3897 (9)	48 (4)
C(3)	4758 (12)	2300 (11)	3554 (8)	56 (5)
C(4)	5434 (9)	1545 (10)	3134 (8)	49 (4)
C(5)	4894 (10)	167 (8)	2339 (9)	49 (4)
C(6)	3745 (12)	−351 (8)	2165 (8)	49 (4)
C(7)	1826 (11)	−135 (8)	2584 (8)	44 (4)
C(8)	1156 (10)	581 (8)	3117 (7)	44 (4)
C(9)	2318 (9)	1576 (7)	−300 (6)	31 (3)
C(10)	1622 (9)	815 (8)	−132 (8)	41 (4)
C(11)	1308 (12)	212 (10)	−780 (10)	60 (5)
C(12)	1701 (13)	282 (8)	−1600 (8)	52 (5)
C(13)	2383 (12)	952 (11)	−1789 (7)	57 (5)
C(14)	2694 (11)	1657 (9)	−1139 (7)	47 (4)
C(15)	4348 (9)	2165 (8)	644 (7)	31 (3)
C(16)	4823 (9)	1374 (7)	291 (7)	33 (3)
C(17)	5978 (10)	1221 (10)	419 (8)	53 (4)
C(18)	6611 (9)	1839 (9)	897 (9)	46 (4)
C(19)	6148 (10)	2617 (10)	1250 (8)	47 (4)
C(20)	5004 (11)	2768 (8)	1108 (8)	41 (4)
C(21)	2660 (9)	3506 (8)	148 (6)	33 (3)
C(22)	3411 (10)	3898 (9)	−425 (8)	49 (4)
C(23)	3256 (12)	4752 (7)	−771 (8)	48 (4)
C(24)	2354 (10)	5282 (7)	−545 (8)	41 (4)
C(25)	1632 (10)	4976 (7)	27 (7)	38 (3)
C(26)	1764 (9)	4035 (7)	387 (7)	34 (3)

[a] Equivalent isotropic U defined as one-third of the trace of the orthogonalized U_{ij} tensor.

$Na[Co(CO)_4]$, NaSMe, KI, and KBr gave the expected substitution products, (η^2-cyclenP)PtLPPh$_3$, where L = $Co(CO)_4$ (**5**), SMe (**6**), I (**7**), and Br (**8**). The bromide reaction is somewhat slower than the iodide reaction (see Experimental Section), as expected on the basis of relative halide binding strengths toward platinum.[10] NMR data for these species are listed in Table IV, and the X-ray crystal structures of **5** and **7** were obtained (see below). The upfield (negative) chemical shift for the cyclenP phosphorus is consistent with its pentacoordinate formulation and is in the usual range found for cyclenPX species when all four nitrogens remain bound to the phosphorus.[3,4,11] The small values of $^2J_{PP}$ in these derivatives indicate that the cis stereochemistry of the phosphorus atoms around platinum is maintained in all cases.[12] NMR spectra for **1**, **7**, and **8** are virtually identical except for slight differences in the phosphorus chemical shifts and one-bond platinum–phosphorus coupling constants. The $^{13}C\{^1H\}$ NMR spectra of these derivatives (see Experimental Section) show the expected four resonances for the cyclen ring, with P–C coupling observed for only two of the carbons.[13] In the ^1H NMR spectrum of **6**, the methyl group appears as an apparent triplet of doublets at δ 2.19, showing both platinum and phosphorus coupling. The IR spectrum (in THF) of **5** shows carbonyl stretching frequencies at 1885 (vs), 1943 (s), and 2018 (m) cm^{-1}, which are at significantly lower frequencies than for other L'Co(CO)$_4$ derivatives.[7,14] This suggests that the Pt–Co bond might be highly ionic in nature, with the $Co(CO)_4$ group bearing a large partial negative charge.

In contrast to anionic Lewis bases, dppm appears to favor PPh_3 displacement. A clean PPh_3 displacement was observed with this potentially chelating ligand to give (η^2-cyclenP)Pt(Cl)dppm (**9**). Although dppm has several binding modes, such as monodentate, bidentate, and bridging, in this case the ligand is monodentate since only one of the phosphorus atoms shows one-bond coupling to the platinum (Table IV). Attempts to displace chloride with $NaBPh_4$ in an effort to chelate the dppm ligand were unsuccessful and led to mixtures of products. This may be due to the formation of oligomers[15] and/or the difficulty of platinum accommodating two rings with acute angles about the metal, ca. 50° for the cyclenP ring and ca. 73° for dppm.[16]

Thus, nucleophiles appear to lead to ligand substitution at platinum, with no obvious involvement of the cyclenP ligand. However, the presence of basic nitrogens on the ligand provides an alternative reactive site for **1** in its reactions with electrophiles. Electrophiles, such as acids and alkyl halides, are known to react with many square-planar platinum(II) complexes and lead to oxidative addition at the metal. We have shown that protic acids prefer ligand, rather than metal, attack (Scheme I) with **1** and anticipated that weaker electrophiles, such as alkyl halides, might also lead to N-alkylation and/or P–N bond cleavage. However, treatment of **1** with MeI or *n*-BuBr led to the halogen-exchange products **7** and **8**, respectively. Such exchange reactions, using alkyl iodides and bromides to displace chloride at platinum, are well documented and known to usually proceed through a platinum(IV) oxidative-addition intermediate, which then undergoes reductive elimination to give the final product.[1] Unfortunately, we found no evidence for *any* intermediate, even at low temperature. Variable-temperature ^1H and ^{31}P NMR spectra showed that the reaction between **1** and MeI did not proceed until about +20 °C; at this temperature only the products, **7** and MeCl, were observed. An alternative to the oxidative-addition/reductive-elimination mechanism in these systems is an N-alkylated species, followed by halide substitution and alkyl halide elimination. In order to see if such a mechanism was plausible, a two-step sequence involving alkylation followed by halogenation was attempted. Methylation of **1** with MeO_3SCF_3 led to [(η^2-MecyclenP)Pt(Cl)PPh$_3$]O_3SCF_3 (**10**), whose cation is the methylated analogue of **3**. The formulation of **10** is supported by the disappearance of the upfield phosphorus chemical shift and the appearance of a downfield one, indicative of P–N bond cleavage and a four-coordinate phosphorus bound to platinum. Although a confident assignment of the methyl resonance in the ^1H NMR spectrum is difficult due to overlapping with the methylene signals, the integrated CH_2/CH_3 vs CH (19:15) regions indicate the presence of the methyl group. In addition, the methyl resonance in the ^{13}C off-resonance decoupled spectrum appears as a quartet (see Experimental Section). The small value of $^2J_{PP}$ again supports the cis arrangement of phosphorus ligands. The product is stable in the solid state but decomposes in solution. Further treatment of **10** with KI yielded **7**.[17] This suggests that the attachment of cyclenP to platinum may yield an alternative pathway to reactions of platinum(II) with electrophiles.

Very weak electrophiles do not appear to react directly with **1**. For example no reaction was observed between **1** and HC≡CPh, even in refluxing THF. However, addition of $NaBPh_4$ to the reaction mixture led to both P–N bond cleavage and Pt–C bond formation, yielding [(η^2-HcyclenP)Pt(C≡CPh)PPh$_3$]BPh_4 (**11**). Breaking of the P–N bond is supported by the large downfield shift of the cyclenP resonance in the ^{31}P NMR spectrum.

(10) Basolo, F.; Pearson, R. G. *Mechanisms of Inorganic Reactions*, 2nd ed.; Wiley: New York, 1967; p 359.
(11) (a) Atkins, T. J.; Richman, J. E. *Tetrahedron Lett.* **1978**, 5149. (b) Richman, J. E.; Atkins, T. J. *Tetrahedron Lett.* **1978**, 4333.
(12) (a) Verkade, J. G. *Coord. Chem. Rev.* **1972/1973**, *9*, 1. (b) Pregosin, P. S.; Kunz, R. W. In *NMR, Basic Principles and Progress*; Diehl, P., Fluck, E., Kosfeld, R., Eds.; Springer-Verlag: Berlin, 1979.
(13) This is in good agreement with the $^{13}C\{^1H\}$ data for **1** in $CDCl_3$ (ppm): 44.7 (d, $^2J_{PC}$ = 15 Hz), 45.3 (d, $^2J_{PC}$ = 10 Hz), 47.4, 50.1.
(14) (a) Pearson, R. G.; Dehand, J. *J. Organomet. Chem.* **1969**, *16*, 485. (b) Hieber, V. W.; Vohler, O.; Braun, G. *Z. Naturforsch.* **1958**, *13B*, 192.
(15) Appleton, T. G.; Bennett, M. A.; Tomkins, I. B. *J. Chem. Soc., Dalton Trans.* **1976**, 439.
(16) Braterman, P. S.; Cross, R. J.; Manojlovic-Muir, L.; Muir, K. W.; Young, G. B. *J. Organomet. Chem.* **1975**, *84*, C40.
(17) This reaction, which yields **7** in moderate yield, may be complicated by several factors. First of all, KI is not soluble in CH_2Cl_2, and no reaction was observed between **10** and KI in this medium, even though **1** and KI do form **7** in CH_2Cl_2. Second, **10** is unstable in solution. Third, as mentioned in the text, group 1 salts with noncoordinating anions (in this case, the expected product KO_3SCF_3) have a tendency to dehalogenate platinum complexes.

Table IV. NMR Data[a]

compd (solv)	^{31}P, ppm ($^{1}J_{PtP}$, Hz) PN	PC	^{1}H, ppm
1 ($CDCl_3$)	−55 (3612) ($^{2}J_{PP}$ = 2)	21 (4702)	2.2–3.6 (comp m, CH_2, 16 H) 7.33, 7.62 (m, CH, 15 H)
3 (CD_2Cl_2)	94 (4497) ($^{2}J_{PP}$ = 19)	13 (3733)	2.3–3.7 (comp m, CH_2, 16 H) 6.06 (br, NH, 1 H, $^{2}J_{PtH}$ = 67 Hz) 7.3–7.7 (m, CH, 15 H)
5 (THF-d_8)	−42 (3331) ($^{2}J_{PP}$ = 10)	23 (4786)	2.3–3.6 (comp m, CH_2, 16 H) 7.38, 7.67 (comp m, CH, 15 H)
6 (THF-d_8)[b]	−24 (2702)	24 (4463)	2.3–3.6 (comp m, CH_2) 2.19 (t d, $^{3}J_{PtH}$ = 30 Hz, $^{4}J_{PH}$ = 6.9 Hz)[c] } 19 H 7.38, 7.67 (comp m, CH, 15 H)
7 (CD_2Cl_2)[b]	−50 (3402)	25 (4686)	2.3–3.7 (comp m, CH_2, 16 H) 7.36, 7.67 (comp m, CH, 15 H)
8 ($CDCl_3$)[b]	−54 (3574)	23 (4691)	2.2–3.6 (comp m, CH_2, 16 H) 7.33, 7.62 (br, CH, 15 H)
9 (THF-d_8)[b]	−50 (3508)	12 (4702) −26 ($^{3}J_{PtPCP}$ = 56) ($^{2}J_{PCP}$ = 77)	2.3–3.7 (comp m, CH_2, 18 H) 7.1–7.3, 7.75 (comp m, CH, 20 H)
10 (CD_2Cl_2)	94 (4492) ($^{2}J_{PP}$ = 12)	11 (3678)	2.1–3.6 (comp m, CH_2, CH_3, 19 H) 7.5, 7.6 (br, CH, 15 H)
11 (CD_2Cl_2)	119 (3055) ($^{2}J_{PP}$ = 21)	10 (3620)	2.3–3.3 (comp m, CH_2, 16 H) 5.81 (br, NH, 1 H, $^{2}J_{PtH}$ = 75 Hz) 6.9–7.7 (comp m, CH, 40 H)

[a] Data for **1** and **3** taken from ref 3b and 3c, respectively. [b] $^{2}J_{PP}$ not observed for cis P atoms. [c] Apparent triplet of doublets due to phosphorus and platinum coupling.

In addition, a new signal in the ^{1}H NMR spectrum appears at δ 5.81 as a broad peak with platinum satellites that integrates to one proton, identical in appearance with the N–H resonance in **3**. The IR spectrum of this compound shows a peak at 2105 cm^{-1}, indicative of a C≡C bond.

The reaction leading to **11** is unusual in two respects. First, both ligand substitution and N-protonation (leading to P–N bond cleavage) is observed. Second, although the use of sodium and/or silver salts with noncoordinating anions is a common method to replace halides at platinum centers, the technique is usually employed to complex weakly coordinating neutral ligands, including π-bonded acetylenes.[1,18,19] However, deprotonation and coordination of terminal alkynes has been reported for platinum group metal chloride complexes with use of a Cu(I) catalyst in the presence of an amine (to deprotonate the alkyne).[20] In the present case, no catalyst is needed and the cyclenP ligand functions as its own internal amine to activate the C–H bond. Several mechanisms are consistent with the formation of **11**. One is Pt–Cl bond rupture, followed by π-coordination of the alkyne and then C–H bond cleavage and rearrangement to a terminal alkyne. Another is N-protonation, followed by displacement of Cl^- by $C{\equiv}CPh^-$. The fact that we found no reaction when **1** was treated with PhC≡CPh and $NaBPh_4$ suggests that the π-bonding mechanism may not be involved in the synthesis of **11** and that N-protonation may occur before alkyne coordination.

The above reactions are summarized in Scheme II and demonstrate not only the remarkable range of reactivity of metal complexes containing the cyclenP ligand but also the selectivity. Thus, anionic nucleophiles displace chloride, while neutral donors favor PPh_3 substitution. Cationic electrophiles with noncoordinating anions attack nitrogen, leading to P–N bond cleavage; those with coordinating anions lead to N–Pt bond cleavage (Scheme I, product **2**). Moreover, the synthesis of **11** shows that, by a suitable choice of reagents, combinations of these reactivities (such as P–N bond cleavage and chloride substitution) can be achieved in one reaction, here leading to the activation of C–H bonds. Although reactions with neutral electrophiles result in ligand exchange at platinum, the mechanism may involve P–N bond breaking and re-forming.

Scheme II

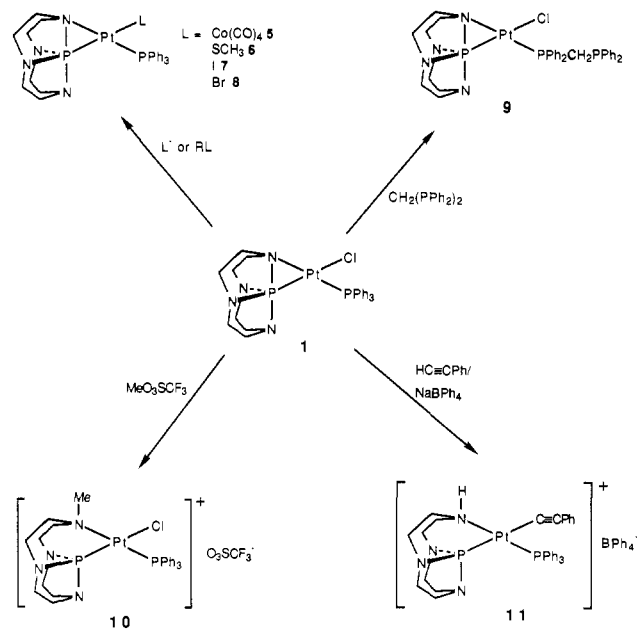

Most of the above derivatives are quite stable, particularly those featuring the P–N–Pt triangular bonding mode. Species **5** is noteworthy since it could serve as an isolable, stable source of $Co(CO)_4^-$. As mentioned above, the low carbonyl stretching frequencies for this derivative indicate a highly ionic metal–metal bond, which should be susceptible to cleavage. In fact, reaction of **5** with Me_3SiI led cleanly to **7** and $Me_3SiCo(CO)_4$.[7] This suggests that other (η^2-cyclenP)PtLPPh$_3$ species, with L = Mn$(CO)_5$, MoCp$(CO)_3$, FeCp$(CO)_2$, etc., may undergo similar reactions.

Structural Descriptions and Comparisons. Selected internuclear distances and angles for **5** and **7** are listed in Table V and their

(18) (a) Michelin, R. A.; Zanotto, L.; Braga, D.; Sabatino, P.; Angelici, R. J. *Inorg. Chem.* **1988**, *27*, 85. (b) Chisholm, M. H.; Clark, H. C. *J. Am. Chem. Soc.* **1972**, *94*, 1532.
(19) Ortho metalation using $AgBF_4$ has also been reported: Avshu, A.; O'Sullivan, R. D.; Parkins, A. W.; Alcock, N. W.; Countryman, R. M. *J. Chem. Soc., Dalton Trans.* **1983**, 1619.
(20) (a) Hiraki, K.; Masumoto, T.; Fuchita, Y.; Zegi, Y. *Bull. Chem. Soc. Jpn.* **1981**, *54*, 1044. (b) Sonogashira, K.; Yatake, T.; Tohda, Y.; Takahashi, S.; Hagihara, N. *J. Chem. Soc., Chem. Commun.* **1977**, 291.

Table V. Selected Bond Lengths (Å) and Bond Angles (deg) for **5** and **7**

Bond Lengths for **5**

Pt–Co	2.751 (2)	Pt–P(1)	2.241 (3)	N(1)–C(5)	1.482 (16)	N(1)–C(12)	1.424 (16)
Pt–P(2)	2.234 (2)	Pt–N(1)	2.123 (8)	N(2)–C(6)	1.441 (15)	N(2)–C(7)	1.464 (14)
Pt–C(1)	2.602 (11)	Pt–C(4)	2.672 (12)	N(3)–C(8)	1.487 (15)	N(3)–C(9)	1.473 (15)
Co–C(1)	1.778 (17)	Co–C(2)	1.789 (17)	N(4)–C(10)	1.488 (16)	N(4)–C(11)	1.418 (16)
Co–C(3)	1.782 (16)	Co–C(4)	1.767 (13)	O(1)–C(1)	1.170 (17)	O(2)–C(2)	1.165 (19)
P(1)–N(1)	1.876 (9)	P(1)–N(2)	1.669 (8)	O(3)–C(3)	1.133 (18)	O(4)–C(4)	1.152 (15)
P(1)–N(3)	1.689 (9)	P(1)–N(4)	1.715 (10)				

Bond Angles for **5**

P(2)–Pt–Co	108.0 (1)	P(1)–Pt–Co	147.9 (1)	N(1)–P(1)–Pt	61.3 (3)	N(1)–P(1)–N(4)	86.8 (5)
P(1)–Pt–P(2)	104.2 (1)	N(1)–Pt–Co	97.1 (3)	N(1)–P(1)–N(3)	178.5 (5)	N(1)–P(1)–N(2)	88.8 (5)
N(1)–Pt–P(2)	155.0 (3)	N(1)–Pt–P(1)	50.8 (3)	P(1)–N(1)–Pt	67.8 (3)	C(5)–N(1)–Pt	117.3 (7)
C(1)–Pt–Co	38.7 (4)	C(1)–Pt–P(2)	101.3 (3)	C(5)–N(1)–P(1)	110.9 (8)	C(12)–N(1)–C(5)	119.7 (10)
C(1)–Pt–P(1)	133.3 (4)	C(1)–Pt–N(1)	98.4 (4)	C(12)–N(1)–Pt	119.8 (8)	C(12)–N(1)–P(1)	111.2 (8)
C(1)–Co–Pt	66.1 (3)	C(2)–Co–Pt	102.8 (4)	C(12)–N(1)–C(5)	118.0 (9)	C(6)–N(2)–P(1)	116.6 (8)
C(2)–Co–C(1)	105.8 (6)	C(3)–Co–Pt	147.2 (6)	C(6)–N(2)–C(7)	116.3 (10)	C(7)–N(2)–P(1)	115.9 (7)
C(3)–Co–C(1)	102.9 (6)	C(3)–Co–C(2)	109.9 (7)	C(8)–N(3)–P(1)	113.9 (8)	C(8)–N(3)–C(9)	116.7 (9)
C(4)–Co–Pt	68.6 (5)	C(4)–Co–C(1)	128.3 (6)	C(9)–N(3)–P(1)	115.7 (8)	C(10)–N(4)–P(1)	110.3 (8)
C(4)–Co–C(2)	107.3 (6)	C(4)–Co–C(3)	101.7 (7)	C(11)–N(4)–P(1)	114.0 (7)	Co–C(1)–Pt	75.2 (5)
N(4)–P(1)–Pt	110.3 (3)	N(3)–P(1)–Pt	119.3 (3)	O(1)–C(1)–Pt	112.1 (9)	O(1)–C(1)–Co	172.7 (10)
N(3)–P(1)–N(4)	91.6 (5)	N(2)–P(1)–Pt	112.9 (3)	O(2)–C(2)–Co	177.8 (14)	O(3)–C(3)–Co	178.3 (16)
N(2)–P(1)–N(4)	127.6 (5)	N(2)–P(1)–N(3)	92.1 (5)	O(4)–C(4)–Co	171.8 (12)		

Bond Lengths for **7**

Pt–I	2.731 (1)	Pt–P(1)	2.236 (3)	N(1)–C(1)	1.481 (16)	N(1)–C(8)	1.455 (13)
Pt–P(2)	2.227 (2)	Pt–N(1)	2.103 (8)	N(2)–C(2)	1.434 (15)	N(2)–C(3)	1.404 (17)
P(1)–N(1)	1.854 (9)	P(1)–N(2)	1.700 (10)	N(3)–C(4)	1.457 (16)	N(3)–C(5)	1.380 (16)
P(1)–N(3)	1.727 (9)	P(1)–N(4)	1.729 (9)	N(4)–C(6)	1.428 (14)	N(4)–C(7)	1.418 (16)

Bond Angles for **7**

P(1)–Pt–I	144.9 (1)	P(1)–Pt–P(2)	110.5 (1)	C(15)–P(2)–C(21)	102.9 (5)	C(21)–P(2)–Pt	118.3 (3)
P(2)–Pt–I	103.7 (1)	N(1)–Pt–I	94.8 (2)	P(1)–N(1)–Pt	68.5 (3)	C(1)–N(1)–Pt	117.7 (7)
N(1)–Pt–P(2)	160.7 (2)	N(1)–Pt–P(1)	50.5 (2)	C(1)–N(1)–P(1)	112.7 (7)	C(8)–N(1)–Pt	117.6 (7)
N(1)–P(1)–Pt	61.0 (3)	N(1)–P(1)–N(2)	87.3 (4)	C(8)–N(1)–P(1)	113.7 (7)	C(8)–N(1)–C(1)	116.9 (9)
N(1)–P(1)–N(3)	175.3 (4)	N(1)–P(1)–N(4)	87.1 (4)	C(2)–N(2)–P(1)	114.1 (8)	C(3)–N(2)–P(1)	111.5 (9)
N(2)–P(1)–Pt	112.8 (3)	N(2)–P(1)–N(3)	91.4 (5)	C(3)–N(2)–C(2)	118.4 (10)	C(5)–N(3)–P(1)	115.1 (9)
N(2)–P(1)–N(4)	129.3 (4)	N(3)–P(1)–Pt	123.6 (3)	C(4)–N(3)–P(1)	112.3 (8)	C(4)–N(3)–C(5)	115.9 (10)
N(3)–P(1)–N(4)	90.2 (5)	N(4)–P(1)–Pt	108.0 (3)	C(7)–N(4)–P(1)	115.5 (8)	C(6)–N(4)–P(1)	110.8 (8)
C(9)–P(2)–Pt	111.9 (3)	C(9)–P(2)–C(15)	104.1 (5)	C(6)–N(4)–C(7)	116.5 (10)		
C(9)–P(2)–C(21)	105.1 (5)	C(15)–P(2)–Pt	113.0 (3)				

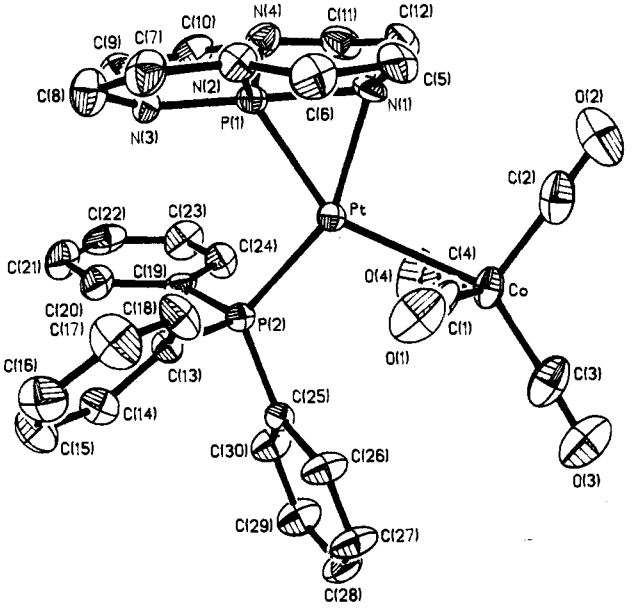

Figure 1. ORTEP drawing of **5** showing the molecular configuration and numbering scheme. Thermal ellipsoids are drawn at the 30% probability level. H atoms are omitted for clarity.

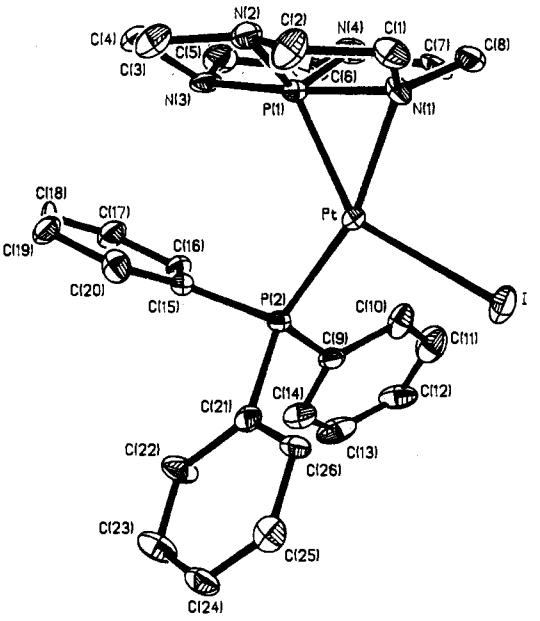

Figure 2. ORTEP drawing of **7** showing the molecular configuration and numbering scheme. Thermal ellipsoids are drawn at the 30% probability level. H atoms are omitted for clarity.

structures illustrated in Figures 1 and 2, respectively. In **7** all four atoms directly bonded to platinum lie virtually in the same plane as the metal atom [sum of cis bond angles is 359.3 (3)°]. Due to the constraint of the three-membered ring the four cis angles each deviate significantly from 90°, with the P(1)–Pt–N(1) angle being only 50.5 (2)°. The geometry about P(1) is distorted trigonal bipyramidal (tbp) with N(1) and N(3) at the axial positions and N(2), N(4), and Pt at the equatorial ones. The N(1)–P(1)–N(3) angle is 175.3 (4)°, while the N(2)–P(1)–N(4) angle is 129.3 (4)°. The three equatorial atoms do not lie in the same plane as P(1) [sum of equatorial angles about P(1) is 350.1 (6)°]. The P(1)–N(1) bond length of 1.854 (9) Å is significantly longer than the other three P–N bonds, which fall in the range 1.70–1.73 Å.

Similar parameters are found for **5** except that the P(1)-Pt-P(2) bond angle is compressed by about 6° in the latter due to the larger steric bulk of the $Co(CO)_4$ ligand. The five-coordinate geometry about Co is best described not as a tbp but as a $Co(CO)_4$ tetrahedron with the Pt atom capping a lower face. Alternatively, the Co geometry could be viewed as a distorted square pyramid (sp) with C(2) at the apical position. The Pt, C(2), and C(3) atoms all lie in the same plane as Co [sum of bond angle is 360 (1)°]. In addition, two of the carbonyls [C(1)-O(1) and C(4)-O(4)] are bent back toward the Pt in an almost semibridging fashion, leading to a slight bending of the Co-C-O angles (about 171°) and Pt-C distances of about 2.6 Å. The other two Co-C-O bond angles are about 178°.[21,22]

Besides the P-N-Pt triangular bonding mode, one of the most unusual features of the Pt complexes **1**, **5**, and **7** is an extremely long Pt-X (X = Cl, I, Co) bond trans to the cyclenP phosphorus [the Pt-Cl distance in **1** is 2.440 (4) Å].[3b] These values are 0.1-0.15 Å longer than typical bonds in related compounds.[23] Spectral measurements also support a weakened Pt-X bond: ν_{PtCl} in **1** is at 249 cm^{-1} [compared to 279 and 303 cm^{-1} in *cis*-$Cl_2Pt(PPh_3)_2$][3b], and as previously noted, the ν_{CO} values in **5** are extremely low. Moreover, once the P-N bond is cleaved, the Pt-X bond length reverts to a normal value [for example, the Pt-Cl bond length in **3** is 2.353 (2) Å]. Long Pt-X bond lengths and low ν_{PtX} values are usually attributed to a strong trans influence of the ligand trans to X; indeed, the Pt-Cl bond length of 2.45 Å and low ν_{PtCl} value of 242 cm^{-1} in *trans*-$ClPt(SiMePh_2)(PMe_2Ph)_2$ were attributed to the large trans influence of Si.[24] However, the trends in these systems cannot be due simply to the pentacoordinated phosphorus since the Pt-Cl bond in **2** (trans to the cyclenP phosphorus) is only slightly lengthened [2.39 (1) Å] and the ν_{PtCl} values are not significantly low (275 and 300 cm^{-1}). Nor is it only the constraint of the three-membered P-N-Pt ring, since the Pt-PPh_3 bond shows no such lengthening. One difference between the pentacoordinate cyclenP ligands in **1** and **2** is its orientation with respect to the platinum coordination plane. In **1**, the N-P-N axial axis of the tbp is in the platinum plane, while in **2** it is perpendicular. This may mean that a tbp phosphorus may be a stronger trans ligand in the former orientation. Support for this comes from the increased cyclenP-Pt bond length in **2** [2.29 (1) Å] compared to 2.22-2.24 Å in the triangular species **3**, **5**, and **7**.

The geometries of cyclenP afford an ideal opportunity to compare the changes in $^1J_{PtP}$ with the three observed coordination modes and are illustrated for **1**, **2**, and **3**. Of particular significance is the observation of $^1J_{PtP}$ for a tbp phosphorus in **2**, a unique monodentate ligand geometry for phosphorus. The phosphorus geometry in **2** is a distorted tbp, with axial and equatorial N-P-N angles of 167 and 115°, respectively; as noted above, the platinum and two equatorial nitrogens are in the same plane as the phosphorus. Thus, the σ-bonding orbital used by phosphorus to bind to platinum is approximately sp^2 hybridized, to a first approximation. This high degree of s character should lead to a large $^1J_{PtP}$ value.[12] Indeed, the observed coupling of 5567 Hz is the largest of any of the derivatives, even though the P-Pt distance is the longest. Cleavage of one P-N bond, as in **3**, results in a more "normal" $R_3P \rightarrow Pt$ binding, with the phosphorus using an approximately sp^3 hybrid orbital. This results in a decrease of about 1000 Hz in the coupling constant. A further 1000-Hz decrease is observed in **1**, which features the P-N-Pt triangular binding mode. This complex is more difficult to treat in a simple hybridization scheme due to the constraints of the three-membered ring. However, the lowering of the coupling constant is consistent with what has been observed before with decreasing chelate ring size: a four-membered ring containing a direct P-Pt bond has a lower coupling constant than a five-membered ring. This has been attributed to angle strain in the smaller ring.[12,16] In **1**, the angle strain is even more pronounced, which should lead to even smaller values. All of the above derivatives have $^1J_{PtP}$ values that fall in the expected ranges, except **11**, for which $^1J_{PtP}$ is only 3055 Hz. Such a diminution of the coupling constant is due to the trans influence of acetylenide ligands.[25]

Acknowledgment. We wish to thank the Robert A. Welch Foundation for generous financial support and Drs. John A. Maguire and John G. Verkade for helpful discussions.

Supplementary Material Available: Tables of anisotropic thermal parameters, bond distances, bond angles, torsion angles, hydrogen atom coordinates, and complete crystallographic data for **5** and **7** (11 pages); tables of observed and calculated structure factors for **5** and **7** (29 pages). Ordering information is given on any current masthead page.

(21) A similar $Co(CO)_4$ geometry was found in the complex *trans*-$(py)_2Pt[Co(CO)_4]_2$ (py = pyridine): Moras, D.; Dehand, J.; Weiss, R. *C. R. Seances Acad. Sci., Ser. C* **1968**, *267*, 1471.

(22) IR spectra in solution and the solid state are very similar (see Experimental Section). The only significant difference between the solid and solution spectra appears to be a more pronounced splitting of one of the bands in the solid state [the shoulder (in THF) at 1920 cm^{-1} is not evident in more dilute solutions]. This suggests that there is little difference between both structures.

(23) See ref 1b for representative Pt-Cl bonds and ref 21 for Pt-Co bonds.

(24) (a) McWeeny, R.; Mason, R.; Towl, A. D. C. *Discuss. Faraday Soc.* **1969**, *47*, 50. (b) Chatt, J.; Eaborn, C.; Ibekwe, S. *Chem. Commun.* **1966**, 700.

(25) For example, for the complexes *cis*-$L_2Pt[P(C_4H_9)_3]_2$, the $^1J_{PtP}$ values are 3500 Hz (L = Cl) and 2219 Hz (L = CCH). See ref 6 and 12b.

Contribution from Rhone-Poulenc, Inc., New Brunswick, New Jersey 08901, and the Department of Chemistry, University of California, Irvine, California 92717

Reactivity of Ceric Ammonium Nitrate with Sodium Cyclopentadienide. X-ray Crystal Structure of $Ce(NO_3)_3(DME)_2$

Peter S. Gradeff,*[1a] Kenan Yunlu,[1a] Timothy J. Deming,[1b] Jeffrey M. Olofson,[1b] Joseph W. Ziller,[1b] and William J. Evans*[1b]

Received November 8, 1988

The reactions of ceric ammonium nitrate (CAN) with 1, 3, 5, and 6 equiv of NaC_5H_5 in THF have been examined. The 6-equiv reaction forms $(C_5H_5)_3Ce(THF)$ in >90% yield in 30-60 min. The 5-equiv reaction forms a cyclopentadienylcerium nitrate complex, $(C_5H_5)_2Ce(NO_3)_2Na(THF)_2$, which decomposes violently upon heating. The 3-equiv reaction forms a cerium(III) nitrate complex of low solubility. A dimethoxyethane (DME) derivative of the latter complex, $Ce(NO_3)_3(DME)_2$, has been characterized by X-ray crystallography. This complex crystallizes from DME at -34 °C in space group $P2_1/n$ with a = 10.4404 (11) Å, b = 15.1301 (21) Å, c = 11.4023 (13) Å, β = 92.431 (9)°, V = 1799.5 (4) $Å^3$, and D(calcd) = 1.87 g cm^{-3} for Z = 4. The reaction of CAN with 1 equiv of NaC_5H_5 causes reduction of Ce(IV) to Ce(III). $(C_5H_5)_3Ce(THF)$ can also be made from $(NH_4)_2Ce(NO_3)_5$ and 5 equiv of NaCp. A scheme describing the overall CAN/NaC_5H_5 reaction system is presented.

Ceric ammonium nitrate (CAN) is a readily available, stable salt of Ce(IV), which is a potentially valuable precursor to a variety of cerium complexes. Recently, for example, the utility of CAN in the preparation of cerium(IV) alkoxides has been demon-

0020-1669/89/1328-2600$01.50/0